

ETH Zürich

Department of Physics

Quantum Device Lab

Semester thesis

Deflection of metastable Helium via Laser light

Author: Dominik Friese

Date: 24th September, 2014

Tobias Thiele

Thesis Advisor

Prof. Dr. A. Wallraff

Principal Investigator

Deflection of metastable Helium via Laser light

Quantum Device Lab
Department of Physics
ETH Zürich
Zurich, Switzerland
September 2014

ABSTRACT

In this thesis the deflection of a collimated beam consisting of metastable 2^3S_1 Helium atoms is investigated.

Various parameters affecting the quality of the beam shape have been varied and optimal parameters were determined.

Furthermore, an outline of the connection to the „Rydberg experiment“ is given.

¹Contact: dfriese@phys.ethz.ch

Table of Contents

1	Introduction	1
2	Theory	2
2.1	Laser Cooling	2
2.2	Collimation & Deflection	5
3	Experimental Set-up	6
3.1	Helium source	6
3.2	Laser setup	7
3.3	Collimation & Deflection	10
3.4	Imaging techniques	12
4	Results	13
4.1	General measurements	13
4.2	Measurements for specific parameters	16
4.2.1	Number of beam splitters	16
4.2.2	Laser power	18
4.2.3	Discharge current	19
4.2.4	Discharge voltage	20
4.2.5	Detuning of the laser	21
5	Conclusion & Outlook	23
5.1	Conclusion	23
5.2	Outlook	23
	Bibliography	27
	Appendix	28

List of Figures

2.1	Laser cooling setup	2
2.2	Net force on the atoms	3
2.3	Energy levels of Helium	4
2.4	Velocity dependent force acting on the atoms	4
2.5	Sketch of the collimation mirror setup	5
3.1	Complete setup of the Helium source	6
3.2	Sketch of the Helium source	7
3.3	Transmission line and population for the saturated absorption spectroscopy	8
3.4	Schematic of the laser setup	9
3.5	Photo of the output setup	10
3.6	Schematic of the beam splitter array	12
4.1	Fit of the background	13
4.2	Two-dimensional MCP image of the background	14
4.3	Two-dimensional MCP image of the collimated beam	14
4.4	Fit of the collimated beam	15
4.5	Relative difference between similar measurements	16
4.6	Deflection comparison between different number of beam splitters	17
4.7	Comparison of different laser beam power	19
4.8	Detuning of the laser	22
5.1	Setup after the deflection	24
5.2	Sketch of the total new setup	25

List of Tables

3.1 Beam splitter array layout	11
4.1 Results for varying number of beam splitters	18
4.2 Comparison of different amplifier diode currents	19
4.3 Comparison of different discharge currents	20
4.4 Comparison of different discharge voltages	20

CHAPTER 1

Introduction

One of the experiments in the Quantum Device Laboratory is the Rydberg experiment. In this experiment metastable Helium atoms are excited to high np Rydberg states with quantum numbers n between 30 and 40. Rydberg atoms are suitable to be introduced in hybrid systems with superconducting qubits or circuits via their large dipole moment. Making use of their possibly long lifetime, they could serve as „Quantum RAM“ in a quantum computer.

So far, the metastable singlet Helium atoms for the Rydberg experiment are produced by a pulsed valve at a rate of 25 Hz which is in turn attached to a regular pressure cylinder filled with He gas. Though, this setup does not give a well collimated beam of atoms.

For a more controlled beam the Helium Source experiment was initiated. Its purpose is to generate a collimated beam of triplet 2^3S_1 -He atoms that is spatially well separated from other states which are also generated in the He source. Out of the resulting beam some atoms are then excited to Rydberg states.

CHAPTER 2

Theory

2.1 Laser Cooling

The idea behind laser cooling is to use the force that light can induce due to a finite photon momentum. Atoms can absorb photons if they carry an amount of energy corresponding to an allowed transition, i. e. they are resonant. Because of the Doppler effect, atoms moving towards or away from the laser source observe a frequency shift of $\delta = \vec{k} \cdot \vec{v}$, where \vec{k} is the photon's wave vector and \vec{v} the atom's velocity. The idea is now to have a laser that is slightly red-tuned with respect to the resonance of the atoms, i. e. it has a lower frequency. This ensures that only atoms with a velocity towards the laser source will absorb photons. To cover all the moving atoms, the laser must impinge them from two opposite sides (in every dimension that is supposed to be cooled). [1]

For a three dimensional cooling one would have a setup similar to Figure 2.1.

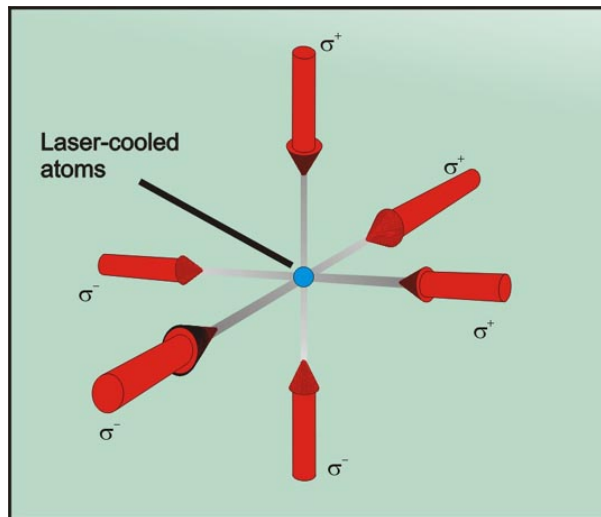


Fig. 2.1: The laser cooling setup. The cooled atoms are placed in the cross section of the lasers. Figure taken from [2].

The net momentum transfer on each atom depends on the rate of both absorption and emission. For lots of emission processes in random directions they cancel each other leaving just the effect of the absorption as seen in figure 2.2.

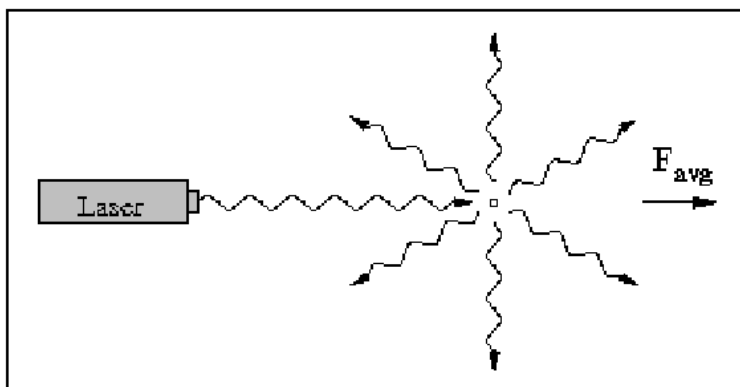


Fig. 2.2: The net force on the atoms. The force from emitted photons cancels for many emissions leaving the force from absorption only. Figure taken from [3].

The total momentum change

$$\Delta\vec{p} = N\hbar\vec{k} \quad (2.1)$$

can be related to a force via

$$\vec{F} = \frac{\Delta\vec{p}}{\Delta t} \quad (2.2)$$

where N is the number of absorbed photons, \vec{k} the wave vector of a single photon and Δt the time in which the absorption happens. To be able to evaluate this expression the $\frac{N}{\Delta t}$ shall be replaced by $\langle \frac{dN}{dt} \rangle$ which is given by the third optical Bloch equation solved in a steady state. For high intensities the force saturates and is given by the expression:

$$\vec{F} = \hbar\vec{k}\frac{\Gamma}{2} \quad (2.3)$$

with Γ being the spontaneous decay rate of the excited state. [4]

In the case of the given experiment the transition $2^3S_1 \rightarrow 2^3P_2$ is used with $\Gamma = 2\pi \cdot 1.62$ MHz and $\lambda \approx 1083.33$ nm. [5]

The 2^3S_1 has a lifetime of ≈ 8000 s and thus can be seen as an effective ground state for the two-level system with the 2^3P_2 state, see Figure 2.3. The laser's bandwidth is narrow enough to avoid stimulation of the transitions to the $J = 0$ or $J = 1$ state.

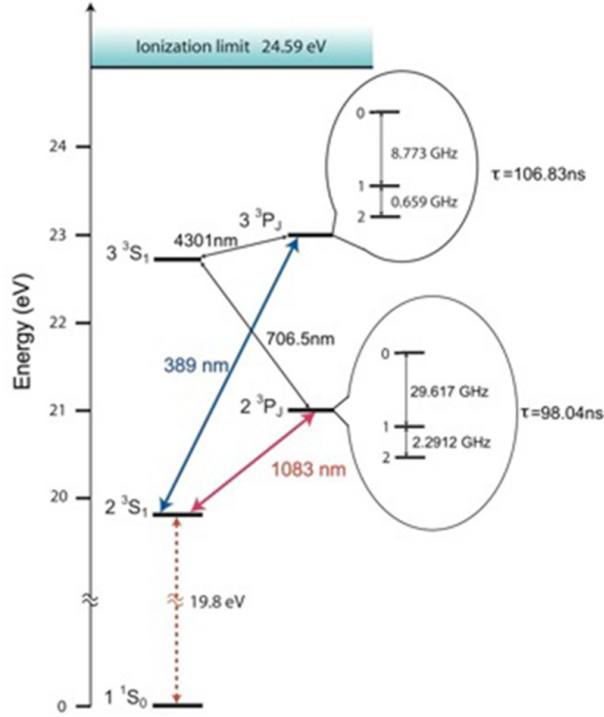


Fig. 2.3: Energy levels of Helium. The transition used in this experiment is marked in red. Figure taken from [6].

For the technique described in section 2.1 there exists a minimal temperature the atoms can be cooled to, called the Doppler limit. It arises from the heating of the atoms by scattering single photons and depends on the natural line-width of the driven transition via

$$T_d = \frac{\hbar\Gamma}{2k_b} \quad (2.4)$$

with Γ as the natural line-width. For the used transition, T_d is about $38.87 \mu\text{K}$. [5]

Altogether, the force is similar to the one given in Figure 2.4 always pushing the atoms towards the center where the resulting force is ideally zero.

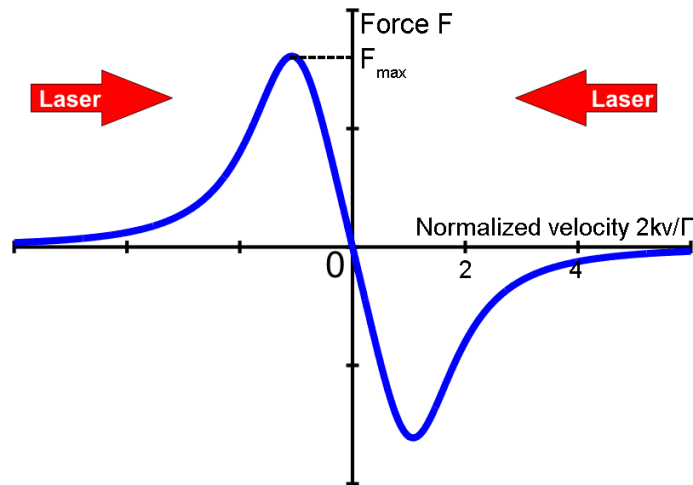


Fig. 2.4: The velocity dependent force acting on the atoms. Units are taken arbitrarily. Figure taken from [1].

2.2 Collimation & Deflection

Both collimation and deflection are based on the principles outlined before. The main difference between the two is that for deflection the laser is applied only from one side, effectively pushing the atoms along the direction of the laser.

It is assumed that the atoms leave the source with a transversal speed of ≈ 18.5 m/s which shall be cooled to ≈ 3 m/s. [5]

For a longitudinal speed of ≈ 1700 m/s and a cooling acceleration of maximal $4.7 \cdot 10^5$ m/s² a minimal cavity length of 6 cm is needed. [5]

Due to decreasing transversal velocity along the propagation axis the angle between laser and beam must constantly be varied. This can be achieved by using two mirrors as seen in Figure 2.5.

The 20 mrad inclination of the laser beam at the beginning of the cavity are optimal for the assumed 18.5 m/s transversal velocity. Ideally, the laser is perpendicular to the atoms at the end of the collimation. A more detailed insight is given in [7].

For the deflection of the metastables we assume a kick of 9 cm/s per photon and an absorption every 200 ns in the best case.

For a deflection length of 14 cm this would lead to absorption of about 400 photons resulting in a velocity of 36 m/s into the desired direction and a separation angle of $\arctan\left(\frac{36}{1700}\right) \approx 1.2^\circ$ between the beams of the metastable and the regular atoms.

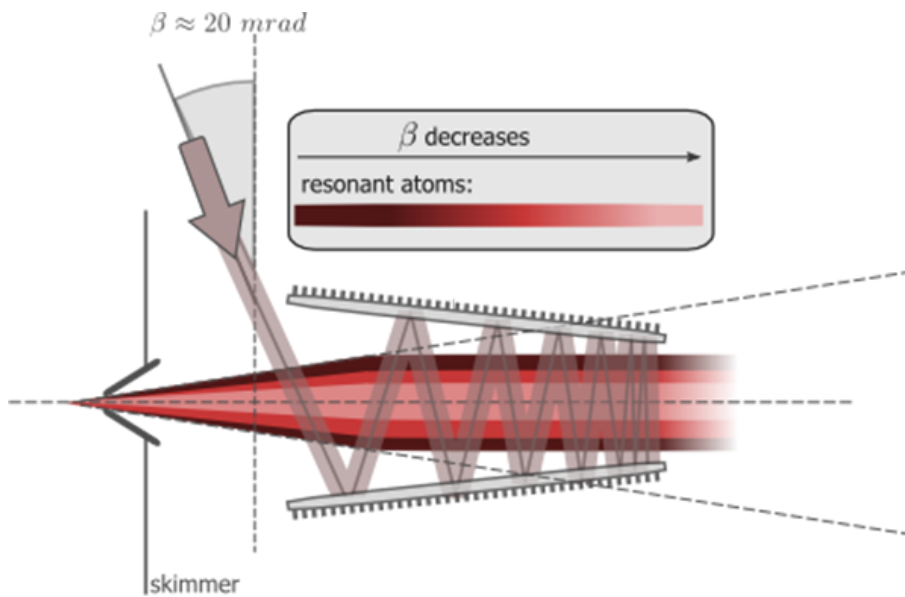


Fig. 2.5: Sketch of the collimation mirror setup. Figure taken from [5].

CHAPTER 3

Experimental Set-up

The complete setup can be seen in Figure 3.1. The colored parts mentioned in the figure are described in the subsequent sections. Furthermore, there are detailed descriptions of the source in the theses of [8] and [7].

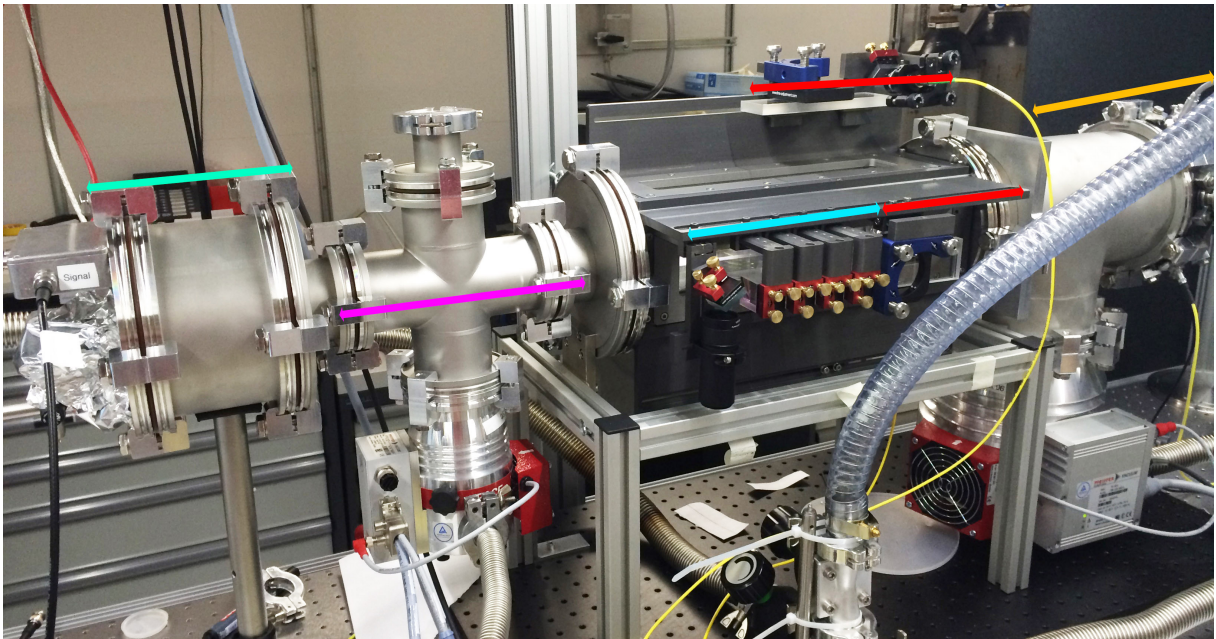


Fig. 3.1: The complete setup except the laser parts described in Section 3.2. Orange is the Helium source explained in section 3.1. Red are the collimation mirrors and laser inputs and blue is the beam splitter array for the deflection, both in section 3.3. Pink is a pump where unwanted atoms are pumped away and green is the detection region with the MCP, see section 3.4.

3.1 Helium source

The source of the Helium atoms consists of a gas cylinder attached to a source chamber containing the pulsed valve similar to the main experiment. [9] The setup is shown in Figure 3.2.

To produce the metastable atom pulses, the following procedure is made use of: Neutral He atoms funnel from the gas cylinder into the discharge chamber accelerating to supersonic speed (in our case around 1700 m/s) and thermalizing to a temperature $T \approx 1\text{K}$

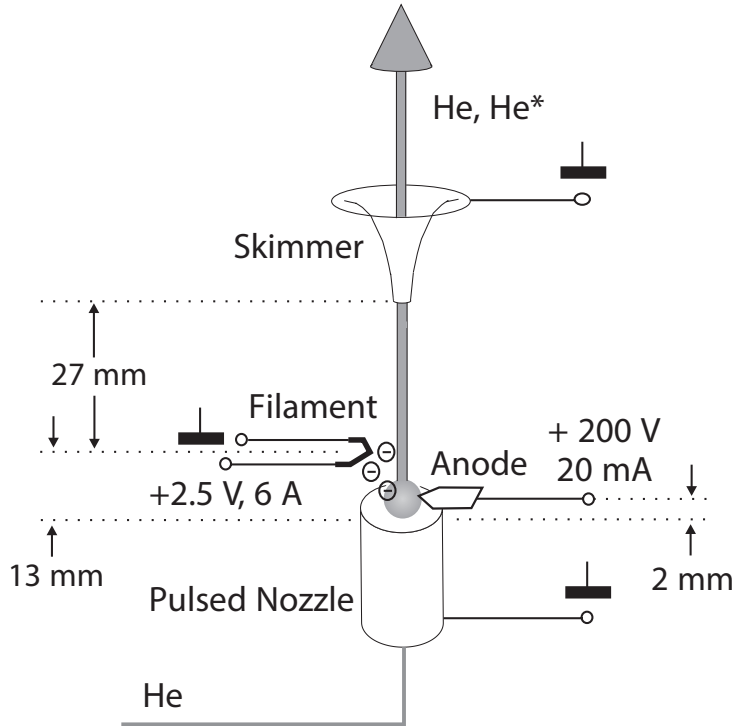


Fig. 3.2: Sketch of the Helium source. Image adapted from [10].

with a repetition rate of 25 Hz.

2 mm beyond the valve a voltage of ≈ 200 V is applied between the valve's nozzle and an anode. This voltage is used to ionize the He atoms to an e^- - He^+ -plasma that moves towards the skimmer. A fraction of about 10^{-6} of the atom-electron pairs recombine into the metastable He^* states whereas the others decay back into the ground state.

Because of the Helium's high ionization potential of 24.59 eV a strong electric field in the range of several kV per mm would be needed to ionize the atoms. To reduce the applied voltage to roughly 200 V additional electrons are inserted via a filament to catalyse the ionization.

A more precise explanation of the procedure is given in [10].

3.2 Laser setup

To be able to control the atomic beam via laser the laser wavelength and hence frequency must be precisely tunable. The laser has the strongest effect on the atoms if it matches exactly the resonance frequency of the given atomic state.

Precise control over the frequency is obtained by the use of a Pound-Drever-Hall lock with an error signal obtained by doppler-free-saturated absorption spectroscopy. The major advantage of this method is the lacking demand of cooling the atoms to a regime where

Doppler broadening of the measured transition frequencies due to the temperature of the atoms is no longer relevant.

The idea is similar to a classical pump-probe method with two beams which traveling in opposite directions. Depending on the relative velocity with respect to one of the beams a different set of atoms absorb the light, i. e. a red-detuned pump beam is absorbed by atoms moving towards the source with a velocity corresponding to the detuning $\delta = \vec{k} \cdot \vec{v}$. The same holds for the probe beam but for the atoms moving away from the source.

For being resonant with one kind of atoms, the pump beam's transmission for the relevant frequency is reduced and the population of the atoms in the upper state is increased as both can be seen in Figure 3.3. The smaller dips in Fig. 3.3 **b)** result from the probe beam whereas the bigger dips are a result of the pump beam. This is called hole burning.

Because of the counterpropagation of the two beams, they address atoms with the same velocity but different direction.

To tune the laser precisely the two dips are 'moved' together to get a transmission spectrum (or equivalently a population profile) similar to the one visible in the second image of Fig. 3.3 **b)** where only one hole is visible. At resonance the condition $\delta = \vec{k} \cdot \vec{v} = \omega - \omega_0$ is satisfied. [11] p. 155 ff.

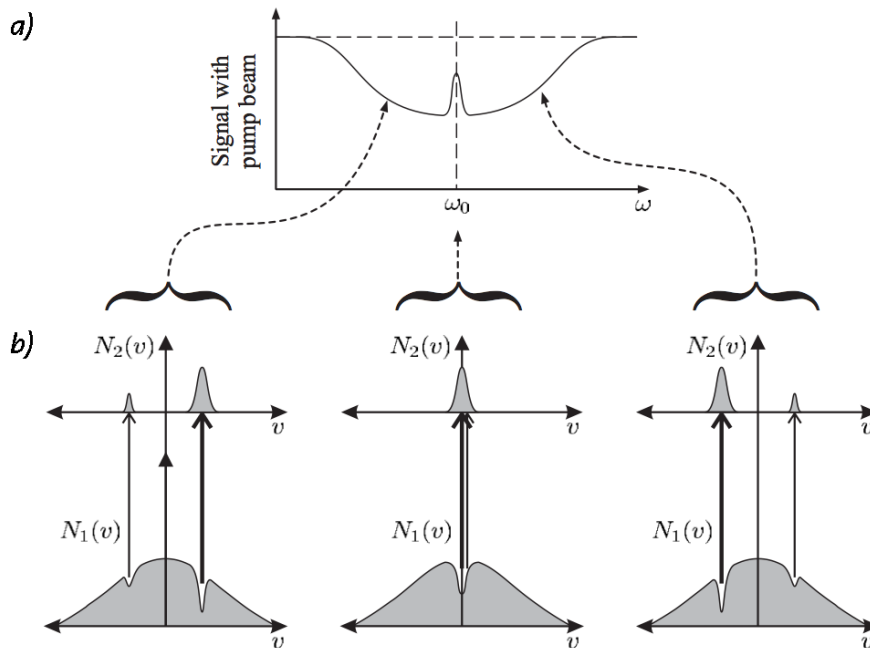


Fig. 3.3: Transmission line and population for the saturated absorption spectroscopy. a) The transmission spectrum of the pump beam with the clearly visible decrease at resonance. b) The population of the ground state N_1 and the excited state N_2 for various detunings. Note that the ground state population can never reach 0 because population inversion is not possible in a two-level system regardless of the beam intensity. Image adapted from [11] p. 158.

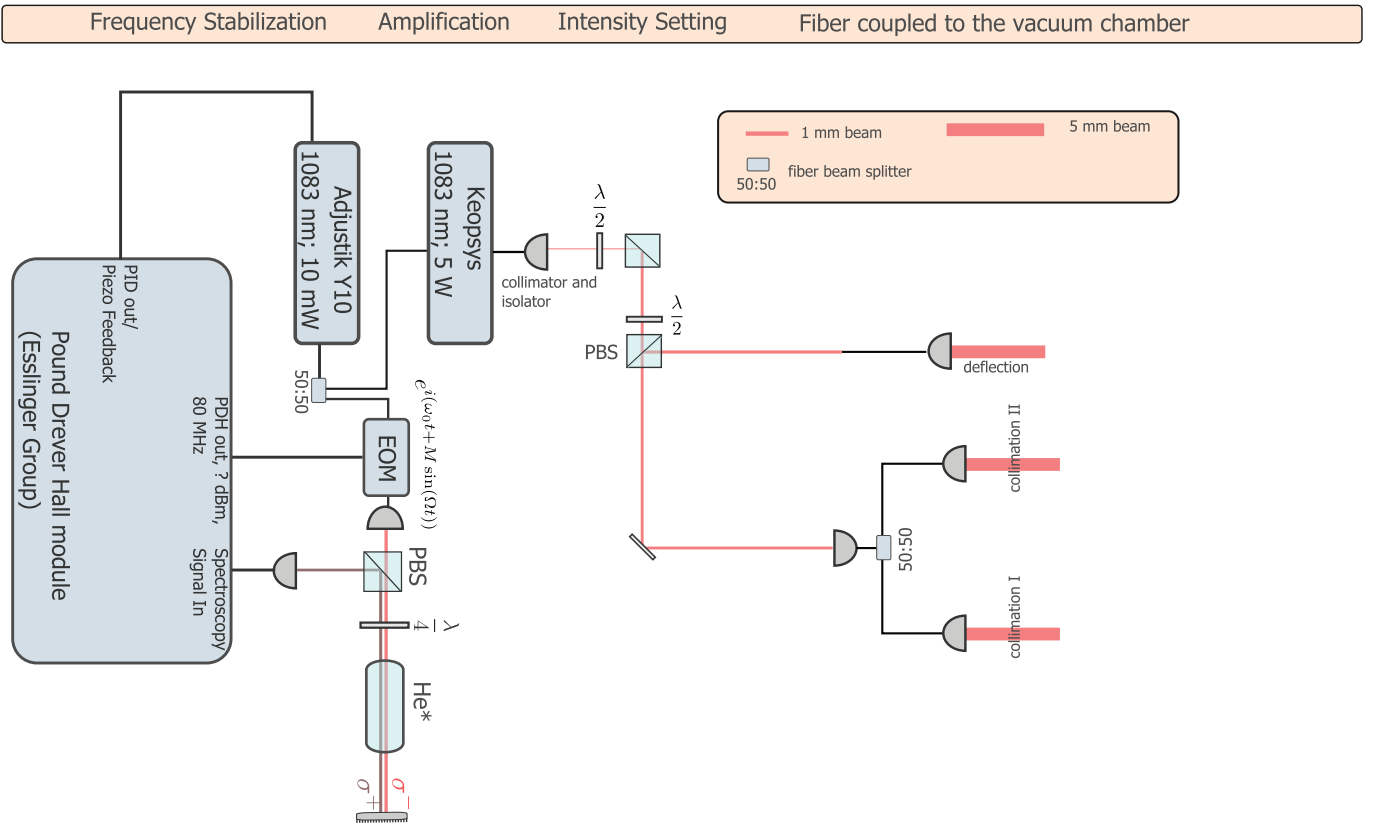


Fig. 3.4: Schematic of the laser setup including laser source, spectroscopy cell (both located at „Frequency Stabilization”), amplification, intensity setting and outputs for deflection and collimation (located at „Fiber coupled to the vacuum chamber”). Figure taken from [5].

To lower the noise, it is important that the two beams have the same frequency. In our case this is realized by re-using the same beam by reflecting it back at the end of the spectroscopy cell instead of splitting it into two parts. Hence one beam acts both as pump and probe beam.

After the laser is stabilized and the frequency is locked correctly it is ready to be used for both collimation and deflection. For the deflection together with the two transversal velocities x and y to be cooled, a total number of three outgoing beams is needed.

The beam setup can be seen in Sketch 3.4 and Image 3.5. The first beam splitter is a polarizing beam splitter and thus the ratio of transmitted and reflected power can be tuned by a $\lambda/2$ plate. In our case we wanted it to be approximately a 75:25 beam splitter. Afterwards a regular 50:50 beam splitter is inserted into the collimation beam path to divide the power equally for both transverse directions.

For suitable collimation a power of 100 mW per direction is adequate whereas the deflection needs a power of at least 700 mW.

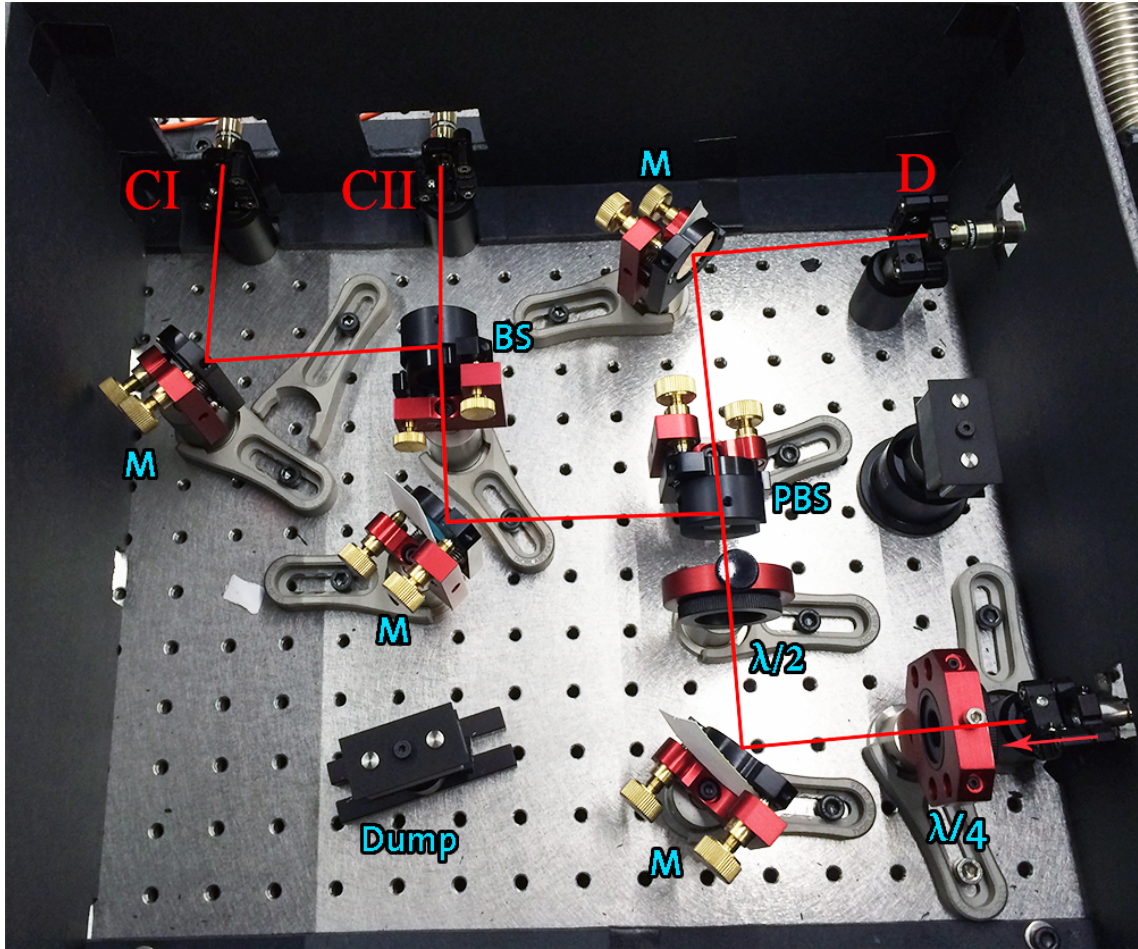


Fig. 3.5: Photo of the output setup. The laser is marked in red and the three beam outputs are denoted by CI and CII for the collimation and D for the deflection. The laser enters the setup from the bottom right signalized by the arrow. Optical parts are denoted in blue with the following meaning: M: mirror, BS: 50/50 beam splitter, PBS: polarizing beam splitter, $\lambda/2$ and $\lambda/4$: respective plates.

3.3 Collimation & Deflection

Collimation

The collimation is done with the laser setup described in the previous section. It enters the chamber both from the top and the left (seen from the beam direction) and is reflected on the opposite sides as shown in Figure 2.5. The corresponding mirrors are attached to the blue mounts visible in Fig. 3.1 marked with the red lines.

The alignment of the mirrors is done via inspection of the MCP's live image. For given laser tuning the mirrors are adjusted such that the collimation is optimal.

A more detailed description and results of the collimation can be found in [7].

Deflection

The deflection is based on the same physics as the collimation with the difference that the laser pushes (i. e. adds momentum to) the Helium beam from only one side – in our case the horizontal direction.

The deflection beam is led through three beam splitters and one mirror to achieve a homogeneous power profile.

The following configuration is used:

Component	Ratio	Relative intensity output
Beam splitter 1	30:70	0.3
Beam splitter 2	30:70	0.21
Beam splitter 3	50:50	0.245
Mirror	100:0	0.245

This setup is optimal for the given beam splitters. Another 30:70 BS would be available but there is no space left to mount it at the experiment.

A sketch of the array can be seen in Fig. 3.6 and a photo in Fig. 3.1. The beam splitters and the laser input are marked with a blue arrow in Fig. 3.1. Ideally, the laser's beam is always perpendicular to the He beam to achieve the best deflection. Since we have a discrete set of mirrors resp. beam directions we can only be perpendicular in four positions. The following beams are supposed to be slightly tilted towards each other to ensure the perpendicularity at each intersection point. The perpendicularity is crucial because the force depends on the angle α between laser and He beam via $F \propto \delta = |k||v| \cos \alpha$ and hence is maximal for an angle of 90° . Also, the effective Doppler width is slightly altered for a non-perpendicular impact and hence less atoms can be affected by the laser.

As before, the theoretical value of 7 mrad for the relative tilting of the beam splitters with respect to each other cannot be adjusted perfectly in coherence and must be optimized by monitoring the beam at the MCP.

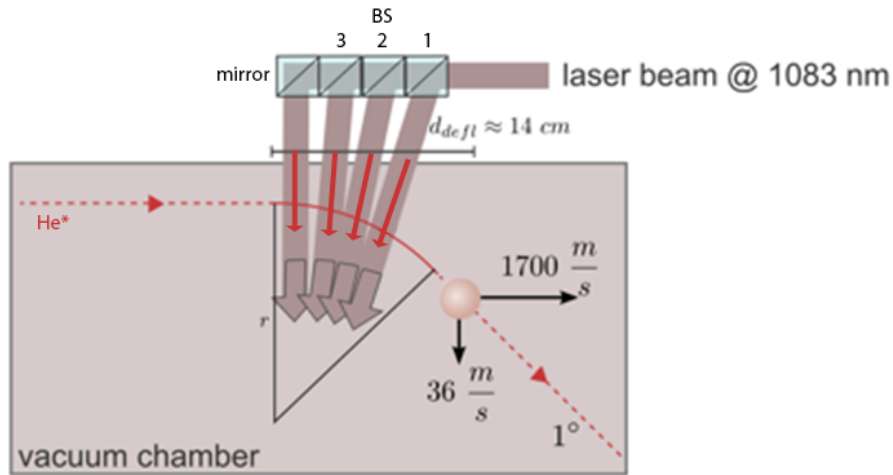


Fig. 3.6: Schematic of the beam splitter array. The deflection laser enters the array from the right where the Helium beam enters the chamber from the left. Ideally, the red arrows are perpendicular to the He* beam. Figure adapted from [5].

3.4 Imaging techniques

The imaging works with a combination of an MCP (micro-channel plate), a phosphor plate and a CCD camera.

Metastable He atoms hit the MCP and knock out electrons which afterwards are multiplied inside the MCP by a factor of $\approx 10^7$. Subsequently, those electrons impinge on a phosphor plate which is stimulated to emit light. This light is then detected by a CCD camera and recorded by the measurement computer.

A more detailed description of the functional principle can be found in [12] p. 5ff and [8] p. 11f.

The camera is set to have an exposure time of 1 s while taking 1 fps.

CHAPTER 4

Results

Several measurement series have been taken to investigate and characterize the system's behavior with respect to various parameters. Practically all data is presented in a way such that the undeflected but collimated beam shape is compared to the deflected one. Additionally, a measurement of the same image but different frame numbers is conducted. At first, some general measurement results, followed by a number of more specific ones, are presented.

4.1 General measurements

Background

In general, both the background and the collimated beam tend to have a Gaussian beam profile. This becomes clear if one has a look at the data for one horizontal or vertical line of the two-dimensional MCP image. The complete image can be seen in Figure 4.2.

From this image each horizontal line is fitted to a Gaussian. The plot for the line with the highest maximum and its corresponding fit can be seen in Figure 4.1.

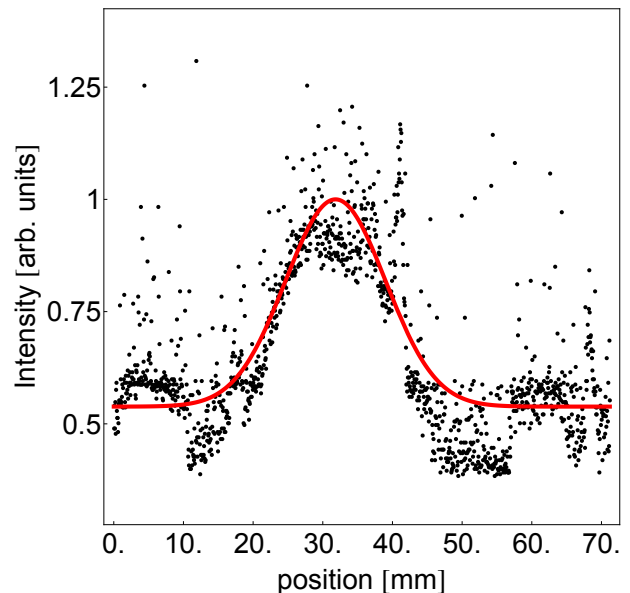


Fig. 4.1: Fit of the background with highest intensity. The ordinate is given in arbitrary units related to the number of counts of metastable He atoms and is normalized to 1.

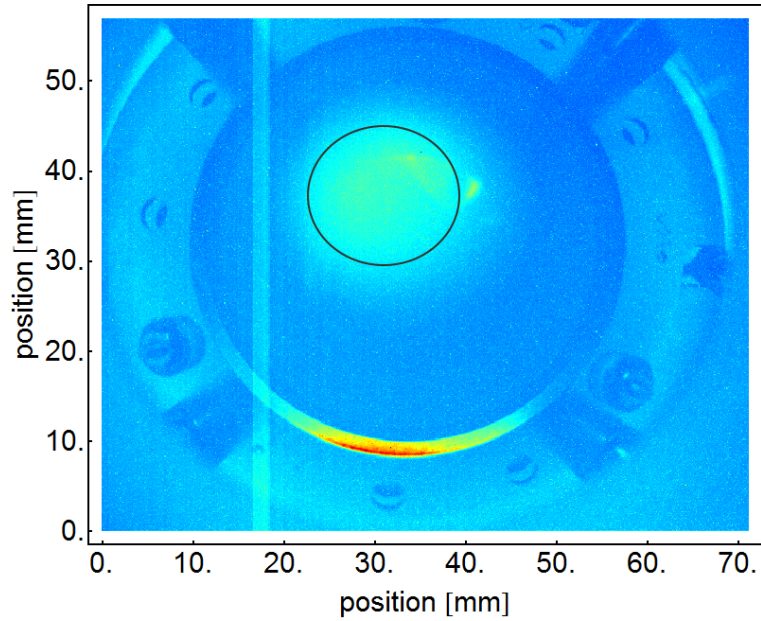


Fig. 4.2: The two-dimensional MCP image of the background. One can see the circular structure of the uncollimated beam due to the round aperture of the skimmer (black circle).

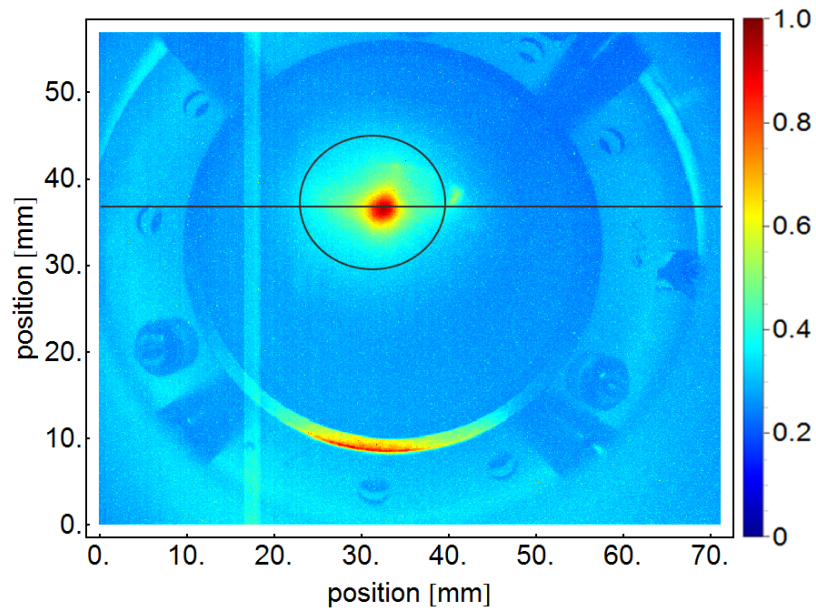


Fig. 4.3: The two-dimensional image of the collimated beam before subtraction of the background. Red coloring represents high intensity whereas blue expresses low intensity. The black line is where I fit the the corresponding function afterwards.

Collimated beam profile without deflection

Figure 4.3 shows the collimated beam at the same color scale as in Figure 4.2.

Comparing the two images, the difference in intensity in the middle where it increases strongly is visible.

To analyze the data, the background is subtracted from the collimated beam and a superposition of a Lorentzian and a Gaussian is fitted into the data to extract the width

and position of the beam easier and more precisely. The corresponding fit for the biggest maximum can be viewed in Figure 4.4.

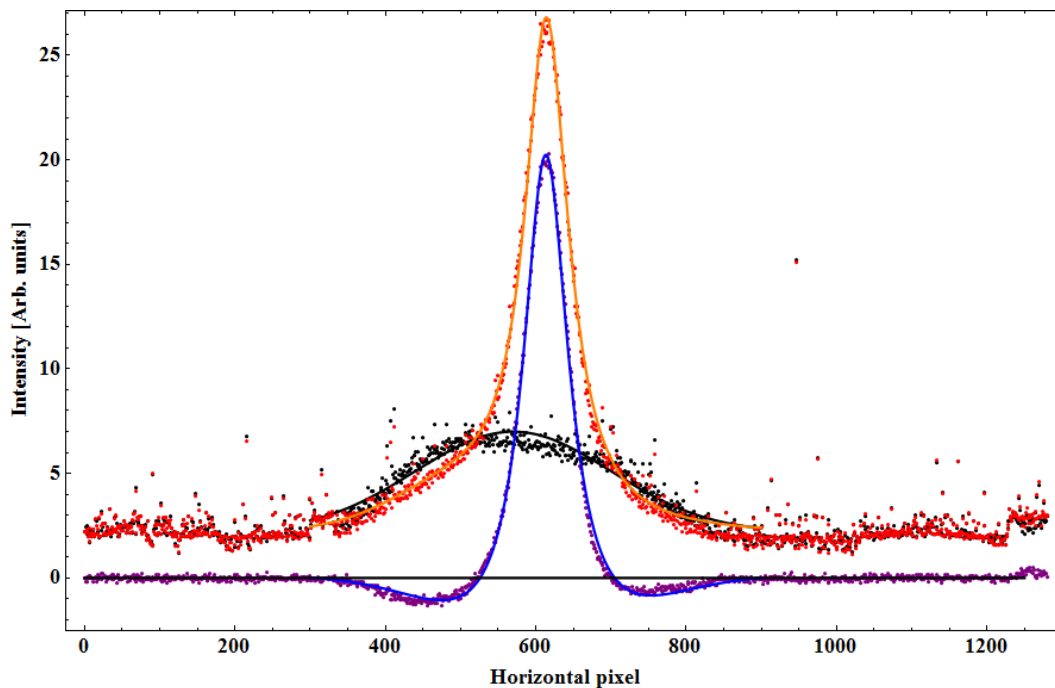


Fig. 4.4: Fit of the collimated beam. The subtracted data has a negative part because atoms are dragged into the middle leaving an effective loss of particles. The fit was made for the horizontal slice marked with the black line in Fig. 4.3

Changing the number of frames averaged

To get an estimate for the impact that the number of averaged frames for one single measurement has, a set of parameters is fixed and the same image is recorded several times with varying average number of frames. Two instances of the same picture for the same number of averages are subtracted and for the resulting data the Frobenius norm of the matrix (the data is given in matrix form) is computed.

In Figure 4.5 the percental difference between two corresponding data sets and an exponential decay are plotted. One can see the decline in difference for higher numbers.

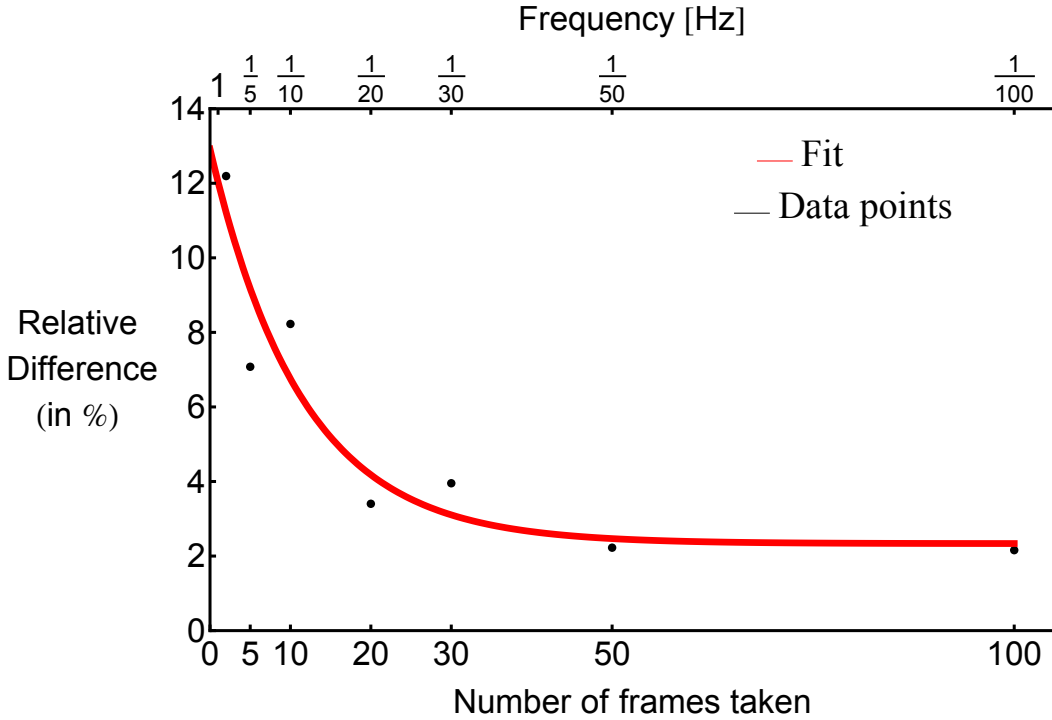


Fig. 4.5: Percental difference between two measurements taken with the same number of frames. Both data points and exponential decay fit are shown.

It can be concluded that taking more than ≈ 50 frames does not result in a gain in accuracy anymore. It just leads to an unnecessary long measurement time due to the exposure of 1 s per frame.

Even using 20-30 frames may be sufficient to have a suitable accuracy.

The fitted error function is $E(t) = a + b e^{-\frac{t}{\tau}}$ with parameters $a = 2.334$, $b = 10.584$ and $\frac{1}{\tau} = 0.0873$ and thus the residual error even for $x \rightarrow \infty$ is approximately 2.33%. Also, we learn from this that the bandwidth of the fluctuations of the valve is on the order of $0.0873 \approx \frac{1}{12}$ Hz.

4.2 Measurements for specific parameters

4.2.1 Number of beam splitters

For this series of measurements the number of beam splitters is changed and the intensity pattern at the MCP is recorded. From this the resulting beam shifts and deflection angles are calculated.

The knowledge gained about the influence of a single beam splitter can be useful to optimize alignment and laser intensity.

As one can see in Figure 4.6 b), the beam is gradually shifted to the left upon adding more

and more beam splitters in a linear way. Furthermore, the beam width is not changed significantly and no tendency can be concluded from Figure 4.6 a).

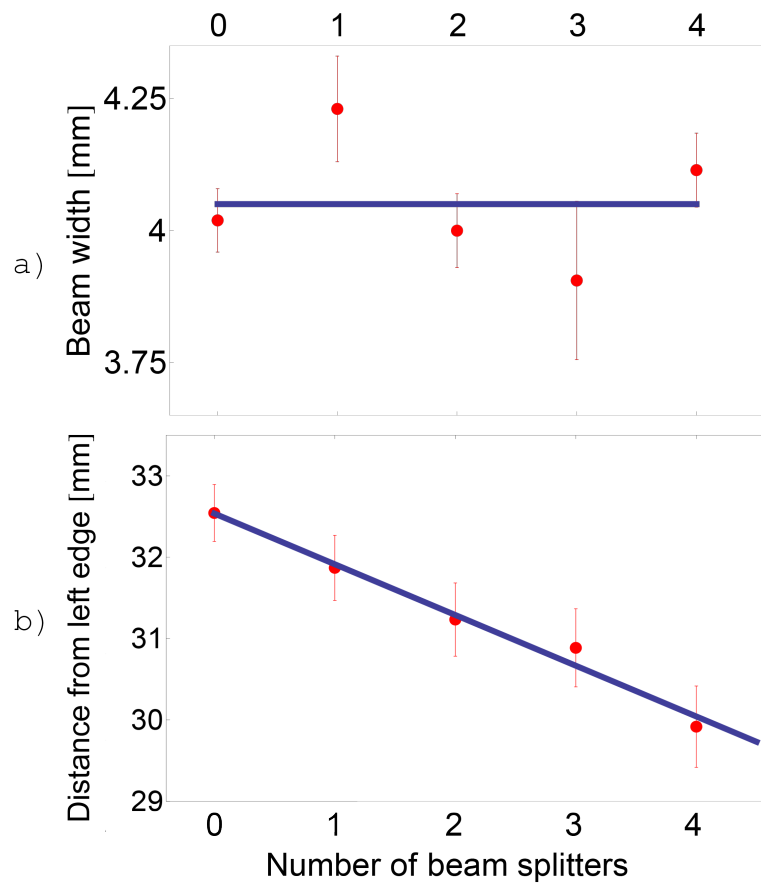


Fig. 4.6: a) The beam width for different number of beam splitters b) Comparison of the deflection distance for different number of beam splitters. The distance is measured from the left edge of the MCP/camera.

In numbers this yields:

Change in # of BS	Difference [mm]	Difference [°]	Photons absorbed
0 → 1	0.674	$0.106 \pm 1.44 \cdot 10^{-3}$	34.95
1 → 2	0.636	$0.100 \pm 1.43 \cdot 10^{-3}$	32.97
2 → 3	0.413	$0.065 \pm 1.35 \cdot 10^{-3}$	21.43
3 → 4	0.969	$0.152 \pm 1.52 \cdot 10^{-3}$	50.11
0 → 4	2.636	$0.413 \pm 1.63 \cdot 10^{-3}$	139.45

Table 4.1: Results for varying number of beam splitters.

Note: The mirror at the end may also be called beam splitter due to simplicity.

The photon number is obtained from simple geometry. The general formula for the absorbed photon number n for i beam splitters used is:

$$n_i = \frac{v_0}{9 \frac{\text{cm}}{\text{s}}} \left[\sin \left(\sum_{l=0}^i \alpha_l \right) - \sum_{l=0}^{i-1} \sin \left(\sum_{m=0}^l \alpha_m \right) \right] \quad (4.1)$$

where v_0 is the initial velocity of $\approx 1700 \frac{\text{m}}{\text{s}}$ and α_l the deflection angle difference with l beam splitters.

As one can see, the number of absorbed photons of ≈ 140 is much less than what was expected. It is smaller than the theoretical value by the same factor as the total deflection differs from the expectations ($\frac{140}{400} \approx \frac{0.413^\circ}{1.2^\circ} \approx 0.34$).

4.2.2 Laser power

The following measurements dealt with the consideration whether the laser's power has an impact on the deflection quality.

All four beam splitters were used and, except from the power, all other parameters were maintained constant.

The laser's power is tuned via the diode current of the amplifier which reaches from 0 mA to 1200 mA. Note that the relation between current and power is non-linear. Thus, one has to draw on the current values when tuning the power. Though, it is possible to measure the laser power directly with a powermeter and fit a function into the data.

As one can see in Figure 4.7 and table 4.2 there seems to be an optimal value for the current resp. the power regarding both the amount of deflection and the beam width being about 800 mA current or 1800 mW total power.

Current [mA]	Power [mW]	Shift [mm]	Shift [°]
0	1100	1.74	$0.27 \pm 1.25 \cdot 10^{-3}$
300	1135	1.73	$0.27 \pm 1.25 \cdot 10^{-3}$
600	1495	1.68	$0.26 \pm 1.27 \cdot 10^{-3}$
900	1915	1.93	$0.30 \pm 1.31 \cdot 10^{-3}$
1000	2043	1.60	$0.25 \pm 1.26 \cdot 10^{-3}$
1200	2303	1.67	$0.26 \pm 1.25 \cdot 10^{-3}$

Table 4.2: Comparison of different amplifier diode currents. The difference is given with respect to the undeflected beam.

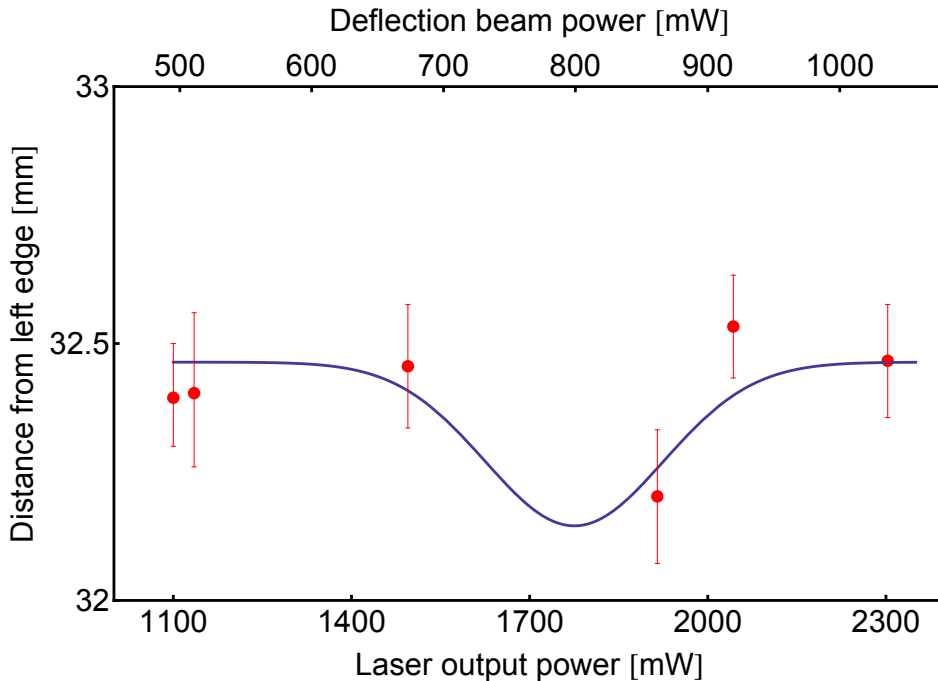


Fig. 4.7: Comparison of different laser beam power. The minimum at 1800 mW (corresponding to ca. 800 mA diode current) is visible.

4.2.3 Discharge current

For this type of measurement the discharge's current was varied.

The effect of the current seems to be tiny regarding the amount of deflection. Needless to say the intensity is strongly increasing with higher discharge current because more and more He atoms remain in the metastable state. Below a certain threshold the current is too low to ionize a sufficient amount of atoms (about 5 A is the minimum value to notice an effect).

To protect the MCP it is not meaningful to use currents above 6 A. Yet for most measurements it is sufficient to be in the 5.50 – 5.75 A realm even though one can observe a slight improvement by going to higher currents as can be seen in Table 4.3.

Current [A]	Shift [mm]	Shift [°]
5.25	2.08	$0.325 \pm 1.31 \cdot 10^{-3}$
5.50	2.12	$0.332 \pm 1.33 \cdot 10^{-3}$
5.75	2.26	$0.353 \pm 1.40 \cdot 10^{-3}$
6.00	2.42	$0.379 \pm 1.43 \cdot 10^{-3}$
6.25	2.51	$0.394 \pm 1.48 \cdot 10^{-3}$

Table 4.3: Comparison of different discharge currents. The difference is given with respect to the undeflected beam.

The shift is slightly increasing as the density of metastables increases with higher discharge current possibly leading to multi-scattering during the deflection. Ultimately, this leads to a greater deflective shift. Nevertheless, a current above 6.0 A should be avoided to prevent the filament from getting damaged.

4.2.4 Discharge voltage

Similar to the variation of the discharge's current one may also change its voltage. In theory, the higher the applied voltage the easier it should be to ionize the atoms.

Voltage [V]	Shift [mm]	Shift [°]
200	1.46	$0.229 \pm 1.28 \cdot 10^{-3}$
230	1.47	$0.230 \pm 1.28 \cdot 10^{-3}$
260	1.46	$0.229 \pm 1.29 \cdot 10^{-3}$
290	1.46	$0.229 \pm 1.27 \cdot 10^{-3}$
320	1.45	$0.227 \pm 1.26 \cdot 10^{-3}$
350	1.45	$0.227 \pm 1.27 \cdot 10^{-3}$

Table 4.4: Comparison of different discharge voltages. The difference is given with respect to the undeflected beam.

Both for the discharge's current and voltage similar observations hold. The intensity undergoes a strong increase and the beam is slightly broadened. However, the change in voltage leads to no improvement of the deflection as can be seen in table 4.4. Thus it is acceptable to operate at a low voltage of 200 V.

Note that the resulting shifts may differ between different measurement series (e. g. sec. 4.2.3 and 4.2.4) because they were taken on different days with different tuning of the laser and collimation settings. Yet the validity of one measurement is not decreased by this.

4.2.5 Detuning of the laser

The detuning of the laser is hard to quantify for the given setup because of the lack of an appropriate reference. Thus the following data is presented phenomenologically to give an impression what it means for the collimation and deflection to be detuned and cannot provide suitable numbers.

The terms ,red' and ,blue' refer to the direction in that the laser was tuned. Left results in a lower wavelength, right in a higher one.

The images given in Figure 4.8 illustrate the outcome of the measurement. From top to bottom the detuning in each direction was increased. Two images in the same row correspond to roughly the same amount of detuning. Also, to be able to compare the images, all plots are normalized to the maximum of the resonance.

As one can see, the collimation is more stable for detuning towards the blue than towards the red but ceases abruptly at a certain point.

For the furthest red-detuning one can see a strip going through the circle indicated by the white dashed lines. The physical origin for that is that atoms are in resonance due to the Doppler shift resulting from their transversal velocity.

Regarding the images themselves it is worth noting that the background was not subtracted to still be able to see the weak signals at all.

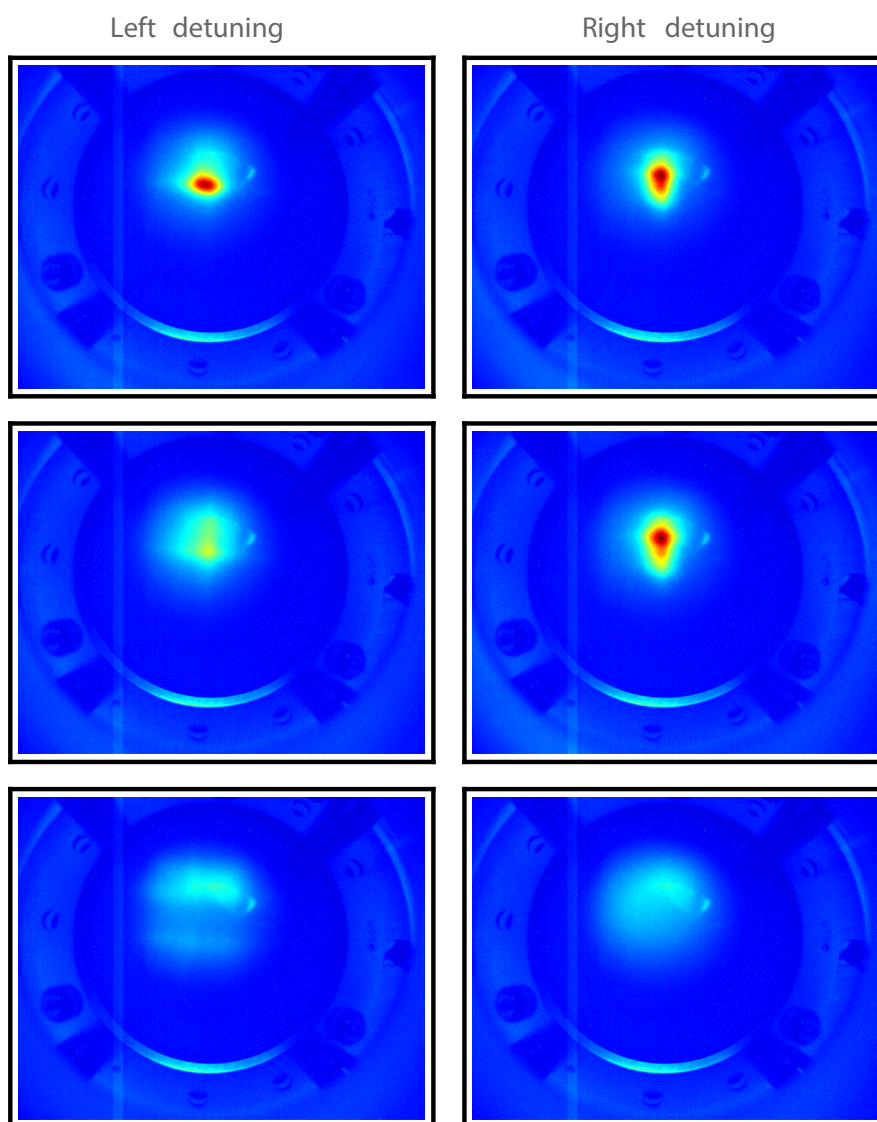
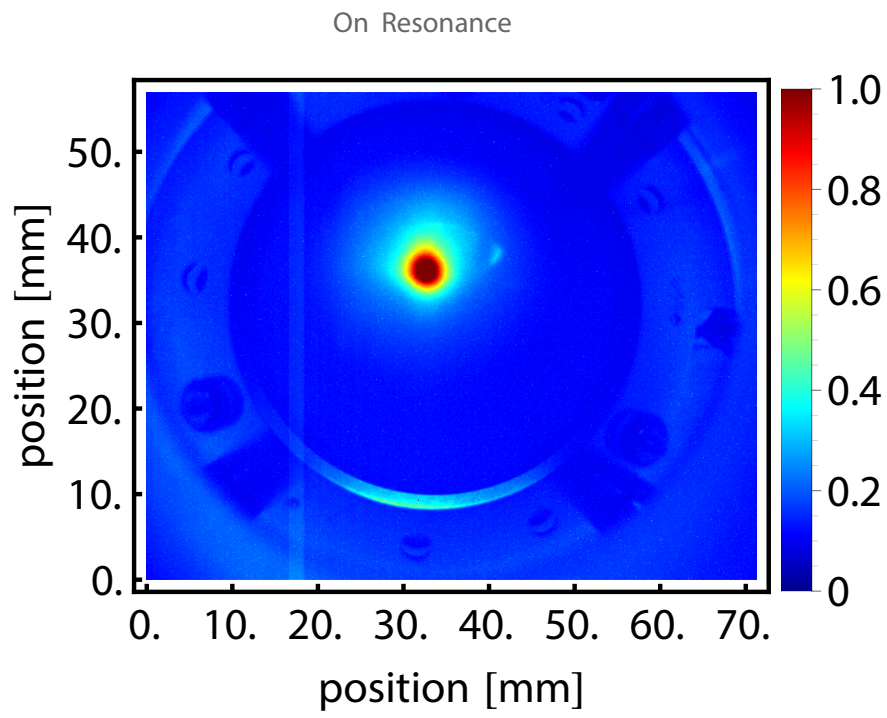


Fig. 4.8: Qualitative comparison for different magnitudes of detuning.

CHAPTER 5

Conclusion & Outlook

5.1 Conclusion

Altogether, the experiment yields a lot of understanding of the source's characteristics and is able to help to improve the Rydberg experiment although not everything worked out as expected. In contrast to the deflection angle of 1.3° calculated beforehand, only 0.45° were achieved which can be accounted to two things: Depressed power broadening of the transmission line and short interaction length.

The power broadening helps to absorb photons over the complete diameter of the deflection laser beam. Without it the resonance would be far too narrow to be able to absorb enough photons to provide a sufficient amount of deflection. The effect of the power broadening can be estimated by consideration of the linewidth: $\Gamma_{\text{broadened}} = \sqrt{1 + s_0} \Gamma$ with $s_0 = \frac{I_{\text{Laser}}}{I_{\text{sat}}}$ and thus $s_0 = \left(\frac{\Gamma_{\text{broadened}}}{\Gamma}\right)^2 - 1$.

For the given data this yields $s_0 \approx 1.94$ and $I_{\text{Laser}} = 1.94 \cdot 0.17 \text{ mW/cm}^2 = 0.33 \text{ mW/cm}^2$ which is far less than what the 'real' intensity is and hence just a lower bound.

Furthermore, we have seen no major change in deflection while increasing the laser power and therefore the depressed power broadening drops out as explanation for the results.

Thus, the short interaction length may be the limiting factor. The deflection angle of 0.45° corresponds to an additional transversal velocity of $\approx 12 \frac{\text{m}}{\text{s}}$ which can be converted to an effective interaction length of 4.5 cm and hence more beam splitters, which is hardly practicable because there is already one beam splitters less in use than in the reference design due to shortage of space, and a bigger laser beam radius could yield better results.

Nevertheless, it is now possible to tune the available parameters such that the source is prepared in a manner that yields an improvement for the Rydberg experiment.

We have seen that the discharge parameters can be set to the minimum values of 200 V and 5.75–6.0 A to protect the components.

For the laser it is crucial that the frequency is well set and the power held between 800 and 1000 mW. Furthermore, the deflection works best for a good collimated beam of about 4 mm width.

5.2 Outlook

Two important questions remain:

- 1) Is the 0.45° deflection angle sufficient to separate the metastable 2^3S_1 -He atoms from the rest?
- 2) How can the new source be attached to the Rydberg experiment?

To solve the first problem one must take a closer look the geometry of the setup. The important parts are shown in Figure 5.1. The dashed orange line results from the residual transversal velocity of the undeflected non-metastable atoms (e. g. ground state He atoms). The distance b between those atoms and the metastables should at least exceed their beam width which was about 4 mm as we have seen in section 4.2.1.

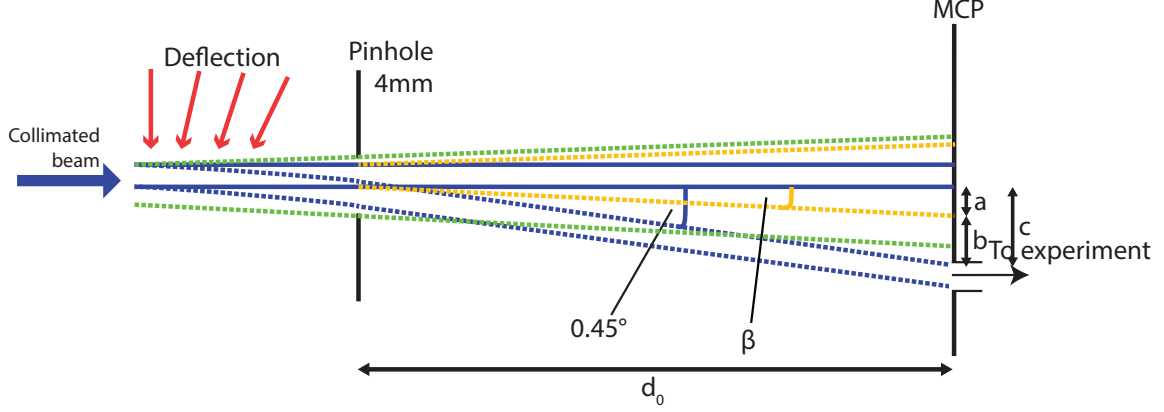


Fig. 5.1: The setup after the deflection. Bold blue is the undeflected beam without spreading, dashed orange is the undeflected beam with spreading from finite residual transversal velocity, dashed green is the beam of uncollimated atoms and dashed blue is the deflected beam of metastable atoms. A pinhole of 4 mm is inserted into the beam path.

To estimate d_0 the following calculation can be done:

$$b = c - a \quad (5.1)$$

$$c = d_0 \cdot \tan 0.45^\circ \quad (5.2)$$

$$a = d_0 \cdot \tan \beta \quad (5.3)$$

The unknown β can be found by some more geometry where the transversal velocity must be guessed. To carry out the calculation it is taken to be $10 \frac{\text{m}}{\text{s}}$.

$$\beta = \arctan \left(\frac{v_x}{v_y} \right) = \arctan \left(\frac{10}{1700} \right) \quad (5.4)$$

All together yields

$$b = d_0 \cdot \left(\tan 0.45^\circ - \frac{10}{1700} \right) \quad (5.5)$$

$$d_0 = \frac{b}{\tan 0.45^\circ - \frac{10}{1700}} \quad (5.6)$$

For a separation b of at least 5 mm we obtain

$$d_0 \approx 1.75 \text{ m} \quad (5.7)$$

Furthermore, one can conclude from equation 5.6 what has to be optimized to get a more compact experimental setup. Favorable are smaller b , larger deflection angle and smaller transversal velocity of the undeflected atoms.

Another important aspect is the separation of the deflected from the uncollimated atoms denoted by the green dashed line. The maximal transversal velocity and the width d_{MCP} of the beam of those atoms is determined by the 2 mm diameter d_s of the skimmer, the 6 mm pinhole d_p and the distance skimmer – pinhole s_{sp} . The numbers give

$$d_{\text{MCP}} = \frac{d_p - d_s}{2 s_{sp}} d_0 = \frac{4}{380} 1750 \text{ mm} \approx 18.42 \text{ mm} \quad (5.8)$$

Thus, the background's atoms nearest to the deflected beam are 9.21 mm off the center. The deflected beam is $c = 13.75$ mm off the center and therefore the d_0 of 1.75 m is sufficient to separate the beams.

The minimum distance d_0 for which the dashed blue and dashed green do not overlap any more can be found by solving the equation

$$d_{0,\text{min}} \cdot \tan 0.45^\circ - 2 \text{ mm} = \frac{2}{380} d_{0,\text{min}} \quad (5.9)$$

And thus

$$d_{0,\text{min}} = \frac{2}{\tan 0.45^\circ - \frac{2}{380}} \text{ mm} \approx 383 \text{ mm} \quad (5.10)$$

which is easier to achieve than the d_0 obtained by the calculation before.

For the second problem a sketch can be seen in Fig. 5.2.

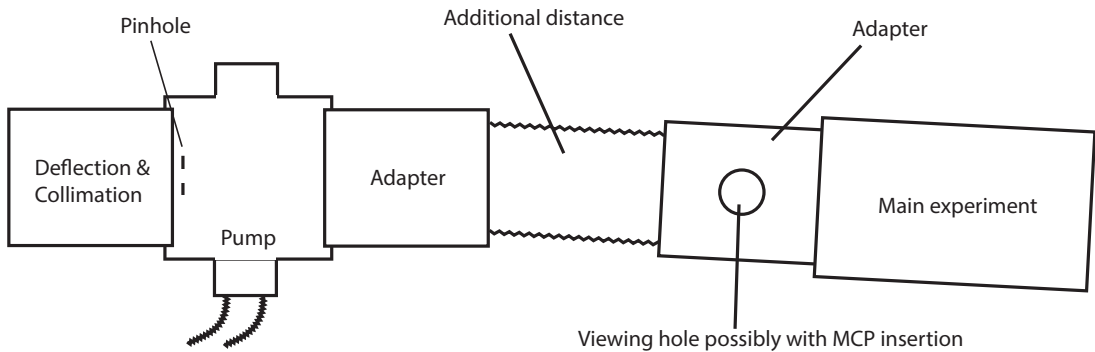


Fig. 5.2: Sketch of the planned joining of the two experiments seen from the top.

The two leftmost parts remain the same as before however the pinhole is inserted into the pump area. The MCP is replaced by a first adapter followed by a regular hose to gain some distance for beam separation. The hose is tilted by the angle of deflection to assist the separation process. After this distance another adapter is located with integrated viewing

holes and possibly a way to insert the MCP. The MCP is crucial in the setup to adjust the source's parameters correctly.

Finally the Rydberg experiment is attached to the adapter at the far right.

Bibliography

- [1] Die freie Enzyklopädie Wikipedia Laser. Laserkühlung.
- [2] Laser cooling basics <http://www.ptb.de/cms/en/fachabteilungen/abt4/fb-44/ag-441/realisation-of-the-si-second/the-atomic-fountain-clock-csf1-of-ptb/laser-cooling-basics.html>.
- [3] Laser Cooling and Optical Molasses, http://ffden-2.phys.uaf.edu/212_spring2007.web.dir/sedona_price/phys_212_webproj_lasercooling.html.
- [4] Tobias Thiele. Towards a Manipulation of Trapped Atoms. 2013.
- [5] Anna Hambitzer. Helium Source 2013: Collimation, Deflection and Spectroscopy. 2013.
- [6] State University New York. He Energy Levels. <http://mysbfiles.stonybrook.edu/~ccorder/Lithography/Lasers.html>, 2014.
- [7] Max Melchner. Collimation of metastable He. 2014.
- [8] Lukas Gerster. Metastable Helium source. 2014.
- [9] Tobias Thiele, Stefan Filipp, Josef Anton Agner, Hansjürg Schmutz, Johannes Deiglmayr, Mathias Stammeier, Pitt Allmendinger, Frédéric Merkt, and Andreas Wallraff. Manipulating Rydberg atoms close to surfaces at cryogenic temperatures. page 12, February 2014.
- [10] T Halfmann, J Koensgen, and K Bergmann. A source for a high-intensity pulsed beam of metastable helium atoms. *Measurement Science and Technology*, 11(10):1510–1514, October 2000.
- [11] Christopher J. Foot. *Atomic Physics*. Oxford, 1st edition, 2005.
- [12] Mario S Könz and Tobias Thiele. Design , Build-up and Control of Electronic Equipment for the Hybrid Rydberg Experiment. 2014.

Appendix

A Mathematica Code

The following code can be used to evaluate measurement data from the Helium source. For given input, various plots, beam width calculations and results for the deflection are provided.

Helium Source;

```
In[1427]:= AxisListFunction[px_] := px / 800 44.5
legendoptions = {LegendMarkerSize -> {35, 30}};
XAxis = Table[AxisListFunction[i], {i, 1, 1280}];
YAxis = Table[AxisListFunction[i], {i, 1, 1024}];
```

I Data Import;

```
Datum = 20140516; (*Enter the date of your measurement here in the format YYYYMMDD*)
foldersave = NotebookDirectory[];

(*Enter the names of your measurement data. The suggestion is to have one file with a non-
deflected (thus just collimated) beam and for each type of deflection one background and one deflected beam file*)
NameList = {"NoDef0.txt", "Background0.txt", "Def0.txt", "Background1.txt", "Def1.txt",
"Background2.txt", "Def2.txt", "Background3.txt", "Def3.txt", "Background4.txt", "Def4.txt"};
folderloadlist = "M:\\Data\\" <> ToString[#] <> "\\HeliumSource\\" & /@ Table[Datum, {i, 1, Length[NameList]}];
data = Import[#, "Table"] & /@ Flatten[Table[folderloadlist[[i]] <> NameList[[i]], {i, 1, Length[NameList]}];
```

2 Plots;

2.1 General Plots;

```
background = 2; (*Index of Background txt file in data*)
NoDef = 1; (*Index of Collimation txt file without Def. in data*)

B0 = 2;
D0 = 3; (*Index of 1st current in data.*)
B1 = 4;
D1 = 5; (*2nd current*)
B2 = 6;
D2 = 7;
B3 = 8;
D3 = 9;
B4 = 10;
D4 = 11;
PlotHeight = 363; (*vertical pixel at which collimation and background plots are taken*)
PlotWidth = 520; (*horizontal pixel at which collimation and background plots are taken*)

(*Can be used to scan through the data and look for high intensities*)
Manipulate[ListPlot[{{XAxis, data[[NoDef]] [[Channel]] - data[[background]] [[Channel]]}~,
{XAxis, data[[D550]] [[Channel]] - data[[background]] [[Channel]]}~}, PlotRange -> {-2.3, 26},
Frame -> True, FrameStyle -> Directive[{Thick, 20}], PlotLegends -> {"No Deflection", "With Deflection
(5.25 A)"}, PlotStyle -> {AbsolutePointSize[3]}, FrameLabel -> {"Position [mm]", "Intensity [arb. unit]"}, ImageSize -> 400,
{{Channel, PlotHeight}, 1, Length[data[[1]]}]]

In[1332]:= BackgroundandCollimation = ListPlot[{data[[NoDef]] [[PlotHeight]], data[[background]] [[PlotHeight]],
data[[NoDef]] [[PlotHeight]] - data[[background]] [[PlotHeight]]}, PlotRange -> {-2, 26}, ImageSize -> Medium];
Export[foldersave <> "BackgroundandCollimation.pdf", BackgroundandCollimation];

In[1334]:= MCPImage = Show[{MatrixPlot[data[[NoDef]], ColorFunctionScaling -> True, ImageSize -> Medium]},
{ListLinePlot[{{0, 0.5 (1024 - PlotHeight)}, {0.5 Length[data[[2, 1]]}, 0.5 (1024 - PlotHeight)}}, PlotStyle -> Black]},
AspectRatio -> 1024 / 1280];
Export[foldersave <> "MCPImage.pdf", MCPImage];
```

2.2 Fits;

(*Fit multiple channels and find maximum intensity over all data. Give back the stripe with maximum intensity. This is used later for the calculations*)

Start with background;

```
In[1336]:= Off[FindMaximum::lstol];
Off[NonlinearModelFit::eit];
GaussFit = a * Exp[-(x - b)^2 / (2 * σ^2)] + c;
lb = 330; ub = 390; (*Upper and lower bound for fitting*)

In[1340]:= BackgroundFit = Table[NonlinearModelFit[data[[background, 1]], GaussFit, {{a, 0.6}, {b, 500}, c, σ}, x], {1, lb, ub}];
Backgroundpar = Table[BackgroundFit[[m]]["BestFitParameters"], {m, 1, Length[BackgroundFit]};
MaximaBG = Table[FindMaximum[{GaussFit /. Backgroundpar[[n]]}, {x, 400}], {n, 1, Length[BackgroundFit]};
LineMaxBG = lb + First@Ordering[Table[MaximaBG[[o, 1]], {o, 1, Length[BackgroundFit]}], -1];

In[1344]:= BackgroundPlot = Show[{ListPlot[data[[1, LineMaxBG + 1]], PlotStyle -> Black}],
  {Plot[GaussFit /. Backgroundpar[[LineMaxBG - lb]], {x, 0, Length[data[[1, lb - 1 + LineMaxBG]]}], PlotStyle -> {Red, Thick}},
  AspectRatio -> 1, Frame -> True, FrameLabel -> {"width[px]", "Intensity[arb. units]",
  LabelStyle -> {13, Bold}, PlotLabel -> "Background", ImageSize -> Medium];
(*Shows Background Intensity at highest peaks px vertically*)
Export[foldersave <> "BackgroundPlot.pdf", BackgroundPlot];
```

Regular data;

(*First without the Deflection*)

```
In[1459]:= GaussFit = a * Exp[-(x - b)^2 / (2 * σ^2)] + c;
NoDefFit = Table[NonlinearModelFit[data[[NoDef, j]] - data[[background, j]],
  {GaussFit, a > 0}, {{a, 14}, {b, 580}, {c, 0.4}, {σ, 30}}, x], {j, lb, ub}];
NoDefpar = Table[NoDefFit[[m]]["BestFitParameters"], {m, 1, Length[NoDefFit]};
MaximaND = Table[FindMaximum[{GaussFit /. NoDefpar[[n]]}, {x, 585}], {n, 1, Length[NoDefFit]};
LineMaxND = lb + First@Ordering[Table[MaximaND[[o, 1]], {o, 1, Length[NoDefFit]}], -1];
PosMaxND = MaximaND[[LineMaxND - lb, 2, 1, 2]]

(*Now with Deflection. Go through all data.*)
D0Fit = Table[
  NonlinearModelFit[data[[D0, j]] - data[[B0, j]], {GaussFit, a > 0}, {{a, 14}, {b, 570}, {c, 0.4}, {σ, 27}}, x], {j, lb, ub}];
D0par = Table[D0Fit[[m]]["BestFitParameters"], {m, 1, Length[D0Fit]};
MaximaD0 = Table[FindMaximum[{GaussFit /. D0par[[n]]}, {x, 575}], {n, 1, Length[D0Fit]};
LineMaxD0 = lb + First@Ordering[Table[MaximaD0[[o, 1]], {o, 1, Length[D0Fit]}], -1];
PosMaxD0 = MaximaD0[[LineMaxD0 - lb, 2, 1, 2]];

D1Fit = Table[
  NonlinearModelFit[data[[D1, j]] - data[[B1, j]], {GaussFit, a > 0}, {{a, 14}, {b, 570}, {c, 0.4}, {σ, 27}}, x], {j, lb, ub}];
D1par = Table[D1Fit[[m]]["BestFitParameters"], {m, 1, Length[D1Fit]};
MaximaD1 = Table[FindMaximum[{GaussFit /. D1par[[n]]}, {x, 575}], {n, 1, Length[D1Fit]};
LineMaxD1 = lb + First@Ordering[Table[MaximaD1[[o, 1]], {o, 1, Length[D1Fit]}], -1];
PosMaxD1 = MaximaD1[[LineMaxD1 - lb, 2, 1, 2]];

D2Fit = Table[
  NonlinearModelFit[data[[D2, j]] - data[[B2, j]], {GaussFit, a > 0}, {{a, 14}, {b, 570}, {c, 0.4}, {σ, 27}}, x], {j, lb, ub}];
D2par = Table[D2Fit[[m]]["BestFitParameters"], {m, 1, Length[D2Fit]};
MaximaD2 = Table[FindMaximum[{GaussFit /. D2par[[n]]}, {x, 575}], {n, 1, Length[D2Fit]};
LineMaxD2 = lb + First@Ordering[Table[MaximaD2[[o, 1]], {o, 1, Length[D2Fit]}], -1];
PosMaxD2 = MaximaD2[[LineMaxD2 - lb, 2, 1, 2]];

D3Fit = Table[
  NonlinearModelFit[data[[D3, j]] - data[[B3, j]], {GaussFit, a > 0}, {{a, 14}, {b, 570}, {c, 0.4}, {σ, 27}}, x], {j, lb, ub}];
D3par = Table[D3Fit[[m]]["BestFitParameters"], {m, 1, Length[D3Fit]};
MaximaD3 = Table[FindMaximum[{GaussFit /. D3par[[n]]}, {x, 575}], {n, 1, Length[D3Fit]};
LineMaxD3 = lb + First@Ordering[Table[MaximaD3[[o, 1]], {o, 1, Length[D3Fit]}], -1];
PosMaxD3 = MaximaD3[[LineMaxD3 - lb, 2, 1, 2]];
```

```

D4Fit = Table[
  NonlinearModelFit[data[[D4, j]] - data[[B4, j]], {GaussFit, a > 0}, {{a, 14}, {b, 570}, {c, 0.4}, {σ, 27}}, x], {j, lb, ub}];
D4par = Table[D4Fit[[m]]["BestFitParameters"], {m, 1, Length[D4Fit]}];
MaximaD4 = Table[FindMaximum[{GaussFit /. D4par[[n]], {x, 575}}, {n, 1, Length[D4Fit]}];
LineMaxD4 = lb + First@Ordering[Table[MaximaD4[[o, 1]], {o, 1, Length[D4Fit]}], -1];
PosMaxD4 = MaximaD4[[LineMaxD4 - lb, 2, 1, 2]];

```

Plot of the fittings;

```

CollimationPlot0 =
  Show[{ListPlot[{data[[NoDef, LineMaxND]] - data[[background, LineMaxND]], PlotStyle → Black, PlotRange → {-2, 20}}],
    {ListPlot[data[[D0, LineMaxD0]] - data[[background, LineMaxD0]], PlotStyle → Blue, PlotRange → {-2, 20}}],
    {Plot[GaussFit /. NoDefpar[[LineMaxND - lb]], {x, 0, Length[data[[1, LineMaxND]]]},
      PlotRange → {-2, 20}, PlotStyle → {Red, Thick}}, {Plot[GaussFit /. D0par[[LineMaxD0 - lb]],
      {x, 0, Length[data[[1, LineMaxD0]]]}, PlotRange → {-2, 20}, PlotStyle → {Green, Thick}}],
    AspectRatio → 1, Frame → True, FrameLabel → {"width[px]", "Intensity[arb. units]"}, LabelStyle → {13, Bold},
    PlotLabel → "Difference from background after collimation", ImageSize → Large];
(*****)
CollimationPlot20 = Plot[GaussFit /. D0par[[LineMaxD0 - lb]],
  {x, 440, Length[data[[1, LineMaxD0]] - 550}, PlotRange → {-1, 130}, PlotStyle → Directive[Thick, Red],
  PlotLegends → Placed[LineLegend[{Style["5.25 A", FontSize → 17]}], legendoptions], {0.8, 0.95}];

CollimationPlot21 = Plot[GaussFit /. D1par[[LineMaxD1 - lb]],
  {x, 440, Length[data[[1, LineMaxD1]] - 550}, PlotRange → {-1, 130}, PlotStyle → Directive[Thick, Blue],
  PlotLegends → Placed[LineLegend[{Style["5.50 A", FontSize → 17]}], legendoptions], {0.8, 0.9}];

CollimationPlot22 = Plot[GaussFit /. D2par[[LineMaxD2 - lb]],
  {x, 440, Length[data[[1, LineMaxD2]] - 550}, PlotRange → {-1, 130}, PlotStyle → Directive[Thick, Green],
  PlotLegends → Placed[LineLegend[{Style["5.75 A", FontSize → 17]}], legendoptions], {0.8, 0.85}];

CollimationPlot23 = Plot[GaussFit /. D3par[[LineMaxD3 - lb]],
  {x, 440, Length[data[[1, LineMaxD3]] - 550}, PlotRange → {-1, 130}, PlotStyle → Directive[Thick, Brown],
  PlotLegends → Placed[LineLegend[{Style["6.00 A", FontSize → 17]}], legendoptions], {0.8, 0.8}];

CollimationPlot24 = Plot[GaussFit /. D4par[[LineMaxD4 - lb]],
  {x, 440, Length[data[[1, LineMaxD4]] - 550}, PlotRange → {-1, 130}, PlotStyle → Directive[Thick, Purple],
  PlotLegends → Placed[LineLegend[{Style["6.25 A", FontSize → 17]}], legendoptions], {0.8, 0.75}];

CollimationPlot2 = Show[CollimationPlot20, CollimationPlot21, CollimationPlot22, CollimationPlot23, CollimationPlot24,
  AspectRatio → 1, Frame → True, FrameLabel → {"position [mm]", "Intensity [arb. units]"}, FrameStyle → Directive[Thick],
  LabelStyle → {23}, PlotLabel → "", ImageSize → 550, FrameTicks → {{{0, 20, 40, 60, 80, 100, 120}, None},
  {{{0, Round[AxisListFunction[0], 0.1]}}, {179.775*2.75, Round[AxisListFunction[179.775*2.75], 0.1]}},
  {179.775*3.75, Round[AxisListFunction[179.775*3.75], 0.1]}}, {179.775*2.5,
  Round[AxisListFunction[179.775*2.5], 0.1]}}, {179.775*3.5, Round[AxisListFunction[179.775*3.5], 0.1]}},
  {179.775*3, Round[AxisListFunction[179.775*3], 0.1]}}, {179.775*4, Round[AxisListFunction[179.775*4], 0.1]}},
  {179.775*3.25, Round[AxisListFunction[179.775*3.25], 0.1]}}, None}},
  Epilog → {Dashed, Black, Line[{{618.1635577119473, 127}, {618.1635577119473, -1}}]}];

Export[foldersave <> "4-curr.pdf", CollimationPlot2];

```

3 Deflection Evaluation;

(*Idea: Calculate the distance between deflected and undeflected beam.

The distances are calculated from the maxima of the corresponding Gauss fits*)

```
In[1495]:= DistanceDefMCP = 366; (*in mm*) (*Total distance between end of deflection cavity and beginning of the MCP*)
```

```

Print["Total Deflection in mm for 5.25 A"]
XDistance0 = Abs[PosMaxD0 - PosMaxND];
YDistance0 = Abs[LineMaxD0 - LineMaxND];
DistanceChan0 = (XDistance0^2 + YDistance0^2)^0.5; (*distance between peaks in "channels"*)
Distancemm0 = AxisListFunction[DistanceChan0] (*distance between peaks in mm*)
(*Umrechnung in Winkel*)
DefAngleRad0 = ArcSin[Distancemm0 / DistanceDefMCP]; (*in Radians*)
DefAngleDeg0 = DefAngleRad0 * 180 /  $\pi$  (*in Degrees*)

Print["Total Deflection in mm for 5.50 A"]
XDistance1 = Abs[PosMaxD1 - PosMaxND];
YDistance1 = Abs[LineMaxD1 - LineMaxND];
DistanceChan1 = (XDistance1^2 + YDistance1^2)^0.5; (*distance between peaks in "channels"*)
Distancemm1 = AxisListFunction[DistanceChan1] (*distance between peaks in mm*)
(*Umrechnung in Winkel*)
DefAngleRad1 = ArcSin[Distancemm1 / DistanceDefMCP]; (*in Radians*)
DefAngleDeg1 = DefAngleRad1 * 180 /  $\pi$  (*in Degrees*)

Print["Total Deflection in mm for 5.75 A"]
XDistance2 = Abs[PosMaxD2 - PosMaxND];
YDistance2 = Abs[LineMaxD2 - LineMaxND];
DistanceChan2 = (XDistance2^2 + YDistance2^2)^0.5; (*distance between peaks in "channels"*)
Distancemm2 = AxisListFunction[DistanceChan2] (*distance between peaks in mm*)
(*Umrechnung in Winkel*)
DefAngleRad2 = ArcSin[Distancemm2 / DistanceDefMCP]; (*in Radians*)
DefAngleDeg2 = DefAngleRad2 * 180 /  $\pi$  (*in Degrees*)

Print["Total Deflection in mm for 6.00 A"]
XDistance3 = Abs[PosMaxD3 - PosMaxND];
YDistance3 = Abs[LineMaxD3 - LineMaxND];
DistanceChan3 = (XDistance3^2 + YDistance3^2)^0.5; (*distance between peaks in "channels"*)
Distancemm3 = AxisListFunction[DistanceChan3] (*distance between peaks in mm*)
(*Umrechnung in Winkel*)
DefAngleRad3 = ArcSin[Distancemm3 / DistanceDefMCP]; (*in Radians*)
DefAngleDeg3 = DefAngleRad3 * 180 /  $\pi$  (*in Degrees*)

Print["Total Deflection in mm for 6.25 A"]
XDistance4 = Abs[PosMaxD4 - PosMaxND];
YDistance4 = Abs[LineMaxD4 - LineMaxND];
DistanceChan4 = (XDistance4^2 + YDistance4^2)^0.5; (*distance between peaks in "channels"*)
Distancemm4 = AxisListFunction[DistanceChan4] (*distance between peaks in mm*)
(*Umrechnung in Winkel*)
DefAngleRad4 = ArcSin[Distancemm4 / DistanceDefMCP]; (*in Radians*)
DefAngleDeg4 = DefAngleRad4 * 180 /  $\pi$  (*in Degrees*)

(*Plot the distances for all currents*)
ListLinePlot[{{5.25, Distancemm0}, {5.50, Distancemm1}, {5.75, Distancemm2}, {6.00, Distancemm3}, {6.25, Distancemm4}},
  PlotRange -> {{5.2, 6.3}, {2.05, 2.55}}, FrameLabel -> {"Current [A]", "Deflection [mm]"}, Frame -> True,
  RotateLabel -> False, PlotStyle -> {Thick, Red}, FrameStyle -> Directive[Thick], LabelStyle -> Directive[14]];

(*Plot the angles for all currents*)
ListLinePlot[{{5.25, DefAngleDeg0}, {5.50, DefAngleDeg1}, {5.75, DefAngleDeg2}, {6.00, DefAngleDeg3},
  {6.25, DefAngleDeg4}}, PlotRange -> {{5.2, 6.3}, {0.32, 0.4}}, FrameLabel -> {"Current [A]", "Deflection angle [°]"},
  Frame -> True, RotateLabel -> False, PlotStyle -> {Thick, Red}, FrameStyle -> Directive[Thick], LabelStyle -> Directive[14]];

```

Comparison to the beam width;

```

Print["Beam width in mm before the deflection"]
AxisListFunction[NoDefpar[LineMaxND - lb, 4, 2]] * 2 * Sqrt[2 Log[2]]
Print[]
Print["Beam width in mm after the deflection"]
AxisListFunction[D600par[LineMaxD4 - lb, 4, 2]] * 2 * Sqrt[2 Log[2]]

```




Eidgenössische Technische Hochschule Zürich
Swiss Federal Institute of Technology Zurich

Declaration of originality

The signed declaration of originality is a component of every semester paper, Bachelor's thesis, Master's thesis and any other degree paper undertaken during the course of studies, including the respective electronic versions.

Lecturers may also require a declaration of originality for other written papers compiled for their courses.

I hereby confirm that I am the sole author of the written work here enclosed and that I have compiled it in my own words. Parts excepted are corrections of form and content by the supervisor.

Title of work (in block letters):

Deflection of metastable Helium via Laser light

Authored by (in block letters):

For papers written by groups the names of all authors are required.

Name(s):

Friese

First name(s):

Dominik

With my signature I confirm that

- I have committed none of the forms of plagiarism described in the ['Citation etiquette'](#) information sheet.
- I have documented all methods, data and processes truthfully.
- I have not manipulated any data.
- I have mentioned all persons who were significant facilitators of the work.

I am aware that the work may be screened electronically for plagiarism.

Place, date

Zürich,

Signature(s)

